

K/π ratios in relativistic heavy ion collisions

C. M. Mader, W. Bauer, and G. D. Westfall

*National Superconducting Cyclotron Laboratory and Department of Physics and Astronomy,
Michigan State University, East Lansing, Michigan 48824*

(Received 11 December 1991)

We calculate the production cross sections for kaons and π mesons in a new hadronic fireball model, which includes all hadrons of masses below 1.3 GeV. We find that we are able to reproduce the increase in the K/π ratios in nucleus-nucleus collisions as compared to proton-nucleus collisions, which was experimentally observed by the E802 Collaboration at Brookhaven National Laboratory. In addition, we predict an isospin effect to be visible in these ratios.

PACS number(s): 25.75.+r

I. INTRODUCTION

A large experimental and theoretical effort is at present being devoted to the search for observables from which the possible formation of a quark-gluon plasma could be deduced. The quark-gluon plasma is envisioned here as a state of matter where quarks and gluons are free to move in a large spatial volume and are not confined to the conventional hadronic color singlets, baryons and mesons. To create this exotic state of matter, high energy densities are needed. These densities may be accomplished by colliding heavy ions at relativistic and ultrarelativistic energies.

Several signals of the formation of a quark-gluon plasma have been suggested. One such signal is the increase in the production of strange particles [1–3]. The simple argument for this enhancement is that in a hadronic environment the minimum center-of-mass energy, \sqrt{s} , for the collision of two particles to result in the production of a KK pair is ≈ 1 GeV, and the minimum \sqrt{s} for the production of any strange particle is ≈ 0.7 GeV via the ΛK channel. In contrast to this, the production of strange particles from a quark-gluon plasma requires only the rest mass of an $s\bar{s}$ quark pair, ≈ 300 MeV.

Specifically, the ratio of kaon to pion production is thought to be a possible signature for the plasma formation [4–6]. Recent experiments have measured pion and kaon spectra in central 14.6 A GeV Si on Au collisions at the Alternating Gradient Synchrotron (AGS) at Brookhaven National Laboratory (BNL). The E802 Collaboration observed that the K/π ratios at midrapidity are substantially greater than those measured in $p + A$ reactions [7,8].

While this enhancement of the K/π ratio is a possible signal of the formation of a quark-gluon plasma, several purely hadronic models have been developed in order to explain the data. Some of the thermal models which have been used include fireball models [9,10], expanding fireball models [11–13], multicomponent firebreak models [14], and Landau fireball models [15,16]. Several hadronic transport model calculations have also been applied to the problem of strangeness production in high energy heavy ion collisions [17–20]. These transport

models are quite successful in reproducing the experimental data [17,21,22], but have to rely on elementary interaction cross sections between the constituents of their models (baryons and mesons or partons or quarks and gluons) which are in some cases not known.

We use the nuclear firebreak model (NFS) [23] which assumes that the colliding heavy ions form a thermalized system. This is not an unreasonable assumption as the experimental data collected at AGS indicate close to full stopping of the heavy ions [24]. Pion spectra have been calculated using the firebreak model for relativistic heavy ion collisions with beam energies (0.4–2.1) A GeV. While the model did a reasonable job of predicting the shape of pion, nucleon, and light fragment spectra, it overpredicted the absolute normalization of the pions. By taking into account the partial transparency of the target nucleus, this overprediction was accounted for [25]. At beam energies around 2 A GeV, the threshold for strange particle production is reached. The firebreak model with corrections for the associative nature of strange particle production [26] was able predict the shape of pion, nucleon, and light fragment spectra. It overpredicted the absolute normalization of the pions, however they did not include the possibility of the target nucleus being partially transparent to the projectile nucleus. Above several A GeV, where densities high enough for the formation of a quark-gluon plasma are believed possible, the transparency and possible production of all mesons and strange baryons with masses below 1.3 GeV are now included in the model. The program now allows for the formation of the π , K , η , $\rho(770)$, $\omega(783)$, $K^*(892)$, $\eta'(958)$, $f_0(975)$, $a_0(980)$, $\phi(1020)$, $h_1(1170)$, $b_1(1235)$, $a_1(1260)$, $f_2(1270)$, $K_1(1270)$, $f_1(1285)$, and $\eta(1295)$. The baryons included in the program are Λ , Σ , and Ξ as well as p , n , and Δ .

II. THE MODEL

The firebreak model of heavy ion collisions [23] assumes that in the region where the target and projectile overlap the nuclear matter reaches thermal and chemical equilibrium. The collision zone is divided into parallel streaks containing a mixture of light fragments, mesons,

and baryons. This gas is treated as a grand canonical ensemble, thus the temperature and chemical potentials of the various types of particles are introduced. These are determined iteratively by equating the average energy, charge, baryon number, and strangeness of the ensemble to the actual energy, charge, baryon number, and strangeness of the streak.

Since the streaks are initially composed of nucleons, the strangeness of the streak is zero. The baryon number is found by

$$B = N_p + N_t, \quad (1)$$

where N_p and N_t are the number of projectile and target nucleons in the streak. Similarly, the charge of the streak is

$$Q = Z_p \frac{N_p}{A_p} + Z_t \frac{N_t}{A_t}, \quad (2)$$

where A and Z are the atomic number and charge of the respective nuclei.

The determination of the thermal energy of the streak is slightly more complicated. The kinetic energy of the

streak is converted to thermal energy through successive nucleon-nucleon collisions. If a streak contains only target or projectile nucleons, then it does not thermalize. Thus only streaks with

$$0 < \eta < 1,$$

where

$$\eta = \frac{N_p}{N_p + N_t}, \quad (3)$$

need be considered.

In some collisions the nucleons are not completely stopped in the center-of-mass frame and the kinetic energy is not completely converted to thermal energy. In order to determine the thermal energy of the streak, the fraction of momentum retained by a nucleon, or transparency, is needed. When a nucleon experiences two-body collisions, its kinetic energy is converted to thermal energy. The average number of nucleon-nucleon collisions a projectile nucleon experiences while traversing the target nucleus is [27]

$$\bar{N}(b) = 2\lambda_p \sigma_{NN} \frac{\int_0^O dx dy \int dz_1 dz_2 \rho_p(x, y + b, z_1) \rho_t(x, y, z_2)}{\int_0^O dx dy \int dz [\rho_p(x, y + b, z) + \rho_t(x, y, z)]}, \quad (4)$$

where σ_{NN} is the energy-averaged total nucleon-nucleon cross section. In practice, we used a value of $\sigma_{NN} = 40$ mb for the calculations at $E/A = 15$ GeV. The xy integration extends over the geometrical overlap O of the two nuclei perpendicular to the beam direction. The factor λ_p is due to Pauli blocking in the final-state phase space of the scattered nucleons. By approximating the initial momentum distributions as Fermi spheres and assuming isotropic angular distribution of the scattering cross section, the fraction of the phase space into which scattering is allowed is

$$\lambda_p = \left[1 - \frac{2p_f^3 - \frac{1}{2}k^2(3p_f - k)}{(p_f + p_b)^3} \right]^2, \quad (5)$$

where p_f is the Fermi momentum of normal nuclear matter, p_b is the beam momentum per nucleon, and

$$k = (p_f - p_b)\theta(p_f - p_b). \quad (6)$$

Using Poisson statistics, the average fraction of center-of-mass momentum a nucleon will retain is then

$$\tau(b) = \exp[-\bar{N}(b)]. \quad (7)$$

The projectile and target streaks are treated independently as streaks with momentum

$$p_i = \pm N_i \tau(b) p_{c.m.} \quad (8)$$

in the center-of-mass frame. This momentum is converted back to a laboratory momentum, thus a laboratory kinetic energy for each streak can be determined. The remainder of the initial laboratory kinetic energy is assumed to be converted to thermal energy and is divided equally among the nucleons in the streak.

In rest frame of the streak, the initial charge, strangeness, baryon number, and energy are determined and must be conserved when the system is in thermal and chemical equilibrium. In a grand canonical ensemble, the momentum distribution for particles with spin S_j , energy E_j , and chemical potential μ_j , in a streak of volume V and temperature T_s , is

$$\begin{aligned} f_j(\mathbf{p}, \eta, b) &= E_j \frac{d^3 N_j}{dp^3} \\ &= E_j \frac{(2S_j + 1)V}{(2\pi)^3} \frac{1}{\exp[(E_j - \mu_j)/T_s](\pm)1} \end{aligned} \quad (9)$$

where the $+$ ($-$) signs stand for fermions (bosons). Integrating this yields

$$N_j = \frac{(2S_j + 1)V m_j^2 T_s}{2\pi^2} \sum_{n=1}^{\infty} \frac{(\mp)^{n+1}}{n} \exp\left[\frac{n\mu_j}{T_s}\right] K_2\left[\frac{nm_j}{T_s}\right] \quad (10)$$

and

$$N_j E_j = \frac{(2S_j + 1) V m_j^3 T_s}{2\pi^2} \sum_{n=1}^{\infty} \frac{(\mp)^{n+1}}{n} \exp\left[\frac{n\mu_j}{T_s}\right] \left[K_1\left[\frac{nm_j}{T_s}\right] + \left[\frac{3T_s}{nm_j}\right] K_2\left[\frac{nm_j}{T_s}\right] \right] \quad (11)$$

in the rest frame of the streak, where K_i , $i=1,2$, is the i th order modified Bessel function of the second kind. In the thermal model, the energy, charge, strangeness, and baryon number densities of the streak are then

$$\begin{aligned} e &= \sum_i \frac{N_i E_i}{V}, \\ q &= \sum_i \frac{N_i Q_i}{V}, \\ s &= \sum_i \frac{N_i S_i}{V}, \\ b &= \sum_i \frac{N_i B_i}{V}. \end{aligned} \quad (12)$$

These are related to the actual values through

$$\begin{aligned} e &= E, \\ q &= Q, \\ b &= B, \\ s &= 0. \end{aligned} \quad (13)$$

These are, however, only four equations, and the temperature, volume, and chemical potentials for all of the different particle types are still unknown.

Since the model assumes each streak is in chemical equilibrium, the chemical potentials can all be related to a linear combination of three chemical potentials. When a streak is in chemical equilibrium, reactions such as



are as likely to occur as their reverse processes. Then

$$\mu_p + \mu_{\pi^-} = \mu_n. \quad (15)$$

For neutral pions, one equilibrium reaction is



therefore

$$\mu_{\pi^0} = 0. \quad (17)$$

In fact, for all nonstrange meson types, M , similar equilibrium conditions apply, yielding

$$\mu_p \pm \mu_{M^\mp} = \mu_n \quad (18)$$

and

$$\mu_{M^0} = 0. \quad (19)$$

The strange mesons and baryons are dealt with in a similar way. The kaons, for example, must be in equilibrium in the following reactions



and



These lead to

$$\mu_{K^0} = -\mu_{\bar{K}^0} \quad (22)$$

and

$$\mu_{K^\pm} = \pm(\mu_p - \mu_n + \mu_{\bar{K}^0}). \quad (23)$$

In this manner, all chemical potentials can be expressed in terms of the neutron, proton, and \bar{K}^0 chemical potentials.

This reduces the number of unknown thermal quantities to five: temperature, neutron, proton, and \bar{K}^0 chemical potentials, and streak volume. Conservation of energy, charge, strangeness, and baryon number will fix four of these values. The constraint that the hadron density equal the freeze-out density, which is the density at which equilibrium ceases, fixes the last quantity through

$$h = \sum_i \frac{N_i H_i}{V} = \rho_c. \quad (24)$$

We can now find T_s , μ_p , μ_n , $\mu_{\bar{K}^0}$, and V by minimizing the function

$$\begin{aligned} \chi(T_s, \mu_p, \mu_n, \mu_{K^0}) &= \left[\frac{h}{\rho_c} - 1 \right]^2 + \left[\frac{e/b}{E/B} - 1 \right]^2 \\ &+ \left[\frac{q/b}{Q/B} - 1 \right]^2 + \left[\frac{s}{b} \right]^2. \end{aligned} \quad (25)$$

Once a thermodynamic description for the streak is known, the invariant cross section for the emitted particles is given by

$$F_j(\mathbf{p}) = \sum_{\eta=0}^1 \int 2\pi b db Y(b, \eta) J_{p' \rightarrow p}(\beta(\eta)) f_j(\mathbf{p}, \eta, b), \quad (26)$$

where $J_{p' \rightarrow p}(\beta(\eta))$ is the Jacobian which transforms from the rest frame of the firestreak with center-of-mass velocity β to the frame of interest. The value of the projectile fraction will range from 0 [$\beta(\eta) = \beta_t$], where there are only target nucleons, to 1 [$\beta(\eta) = \beta_p$] where there are only projectile nucleons. f_j is the invariant momentum distribution of a particle of type j and momentum \mathbf{p} , produced in a streak with energy E , and projectile fraction η . For particles produced in the streak, this is given by Eq. (9). For particles which are products of the decay of resonances created in the streak,

$$f_j(\mathbf{p}, \eta, b) = \sum_F \frac{W_D(2S_R+1)Vm_R T_s^2}{(2\pi)^3 p p_D} \left[\frac{\mu_R}{T_s} \ln \left[\frac{1+e^{x_-}}{1+e^{x_+}} \right] + \sum_{n=1}^{\infty} \frac{(\mp)^{n+1}}{n^2} [e^{-nx} - (nx_- + 1)e^{-nx} + (nx_+ + 1)] \right], \quad (27)$$

where

$$x_{\pm} = \frac{m_R}{m_j^2 T_s} (EE_D \pm p p_D) - \frac{\mu_R}{T_s}. \quad (28)$$

W_D is the branching ratio for the decay of a resonance of type R into a particle of type j . The energy and momentum of the decay product in the rest frame of the resonance are E_D and p_D , respectively. The yield function $Y(b, \eta)$ is given by

$$Y(b, \eta) = \int_{\eta-(1/2)\delta\eta'}^{\eta+(1/2)\delta\eta'} d\eta' \int dx dy dz \delta(\eta' - \eta_b(x, y)) [\rho_p(x, y + b, z) + \rho_t(x, y, z)], \quad (29)$$

where $\rho(r)$ is the diffuse radial density distribution [23]

$$\rho(r) = \begin{cases} \rho_0 \left[1 - \left[1 + \frac{R}{a} \right] \exp \left[-\frac{R}{a} \right] \frac{\sinh(r/a)}{r/a} \right], & r \leq R \\ \rho_0 \left[\frac{R}{a} \cosh \left[\frac{R}{a} \right] - \sinh \left[\frac{R}{a} \right] \right] \frac{\exp[-(r/a)]}{r/a}, & r \geq R \end{cases} \quad (30)$$

with R and a given by $1.2A^{1/3}$ and $\sqrt{1/2}$, respectively.

In the original model, where the transparency was independent of b , f_j was also independent of impact parameter allowing Eq. (26) to be rewritten as

$$F_j(\mathbf{p})|_{\text{orig}} = \sum_{\eta=0}^1 Y_{\eta} J_{p' \rightarrow p}(\beta(\eta)) f_j(\mathbf{p}, \eta), \quad (31)$$

where Y_{η} is the impact parameter integrated yield function

$$Y_{\eta} = \int 2\pi b db Y(b, \eta). \quad (32)$$

In our present model, Eq. (26) is solved numerically using Eqs. (9), (27), and (29), using the temperature, volume, and chemical potentials found by minimizing Eq. (25). The result is the prediction of the triple-differential invariant cross sections for the particle species considered.

III. PARTICLE PRODUCTION IN THE MODEL

Experimental measurements have shown the K/π ratios increase with the mass of the colliding system [8]. The yield of kaons with strangeness $+1$ (which contain \bar{s} quarks) is always higher than the yield of their antiparticles. In order to try and understand this we looked at how various aspects of our model affected particle production.

For any particle, if its chemical potential is zero, then the yield of the particle is equal to the yield of its antiparticle. The kaons with positive strangeness have positive chemical potentials in all cases and their yields are always larger than their antiparticle. The nonzero chemical potential is due to the different production mechanisms for strange mesons and their antiparticles. If strange mesons were only produced in pairs (e.g., K^+K^- , $K^+\bar{K}^0$, $K^0\bar{K}^0$),

then $\mu_{K^+} = 0$. However, there are also associative production processes. For the mesons with strangeness $+1$, there are processes involving hyperons of strangeness -1 and -2 . For example,

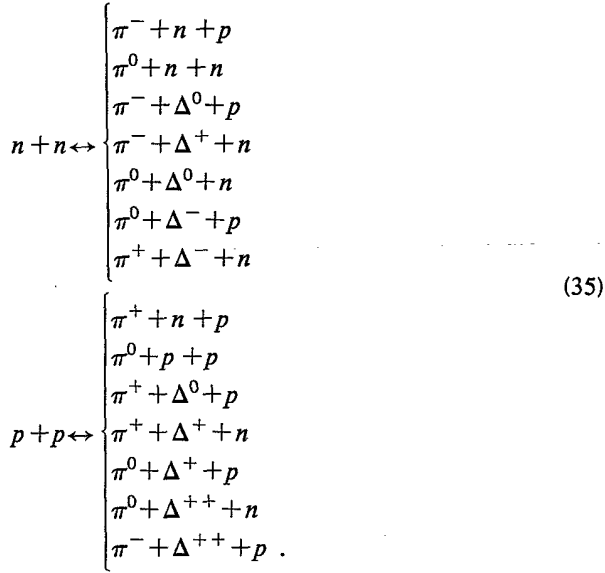
$$p + p \leftrightarrow \begin{cases} K^+ + \Lambda + p, \\ K^0 + \Sigma^+ + p, \\ K^+ + K^+ + \Xi^- + p. \end{cases} \quad (33)$$

Associative production of mesons of strangeness -1 involves antibaryons. For the negative kaon,

$$\bar{p} + n \leftrightarrow K^- + \bar{\Lambda} + n \quad (34)$$

is a possible process. Antibaryon cross sections are about two orders of magnitude less than the corresponding baryon cross sections, so particles with positive strangeness are more abundant than their antiparticles and $\mu_{K^+} > 0$.

If transparency is not included, then the temperature and chemical potentials in the streaks are dependent only on N/Z of the system and the beam energy per nucleon. For $N=Z$ nuclei, in central $14.6A$ GeV symmetric collisions, $T_s = 127.4$ MeV, $\mu_{\pi^+} = -0.3$ MeV, and $\mu_{K^+} = 46.5$ MeV. The pion chemical potential is nonzero due to the difference in the neutron and proton masses. If $N > Z$, as in Au on Au collisions, the temperature is unchanged, however, μ_{π^+} and μ_{K^+} both decrease. This leads to $\pi^+/\pi^- < 1$. Similarly, in $p+p$ reactions, $N < Z$, thus $\mu_{\pi^+} > 0$ and $\pi^+/\pi^- > 1$. This can be explained by looking at the possible pion production reactions for both $n+n$ and $p+p$. The contributions of the following reactions are the most significant in pion production:



There are three times as many ways to directly produce thermal π^- as π^+ in neutron collisions. The opposite is true for proton reactions. In Table I, the yields of charged kaons and pions are shown for several central 14.6A GeV symmetric collisions. For all of these reactions, $\approx 60\%$ of the pions produced are thermal and in fact, $\pi^\mp/\pi^\pm > 3$ in neutron and proton systems, respec-

TABLE I. Probability per nucleon in a streak for producing charged pions and kaons in central $A + A$ ($\eta=0.5$) collisions at 14.6A GeV/c. The % yields for direct and decay production are also included.

	$n+n$	$p+p$	He+He	Au+Au
K^+	0.112	0.145	0.151	0.158
% thermal	87.20	90.77	88.44	87.87
% K res	9.38	6.59	8.19	8.55
% ϕ	3.42	2.64	3.37	3.58
K^-	0.063	0.049	0.072	0.082
% thermal	87.50	83.20	85.06	85.32
% K res	6.37	8.96	7.89	7.79
% ϕ	6.13	7.84	7.05	6.89
π^+	0.493	0.868	0.769	0.787
% thermal	63.03	68.36	66.08	65.78
% Δ	12.67	15.04	12.26	11.32
% ρ	14.36	10.96	13.55	14.20
% other	9.94	5.64	8.12	8.69
π^-	0.872	0.494	0.772	0.866
% thermal	68.39	63.08	66.12	66.84
% Δ	15.06	12.69	12.27	11.69
% ρ	10.94	14.33	13.53	13.58
% other	5.62	9.90	8.08	7.90
K^+/K^-	1.79	2.96	2.09	1.93
π^+/π^-	0.565	1.76	0.996	0.908
K^+/π^+ (%) (%)	22.7	16.7	19.6	20.1
K^-/π^- (%) (%)	7.17	9.89	9.36	9.46

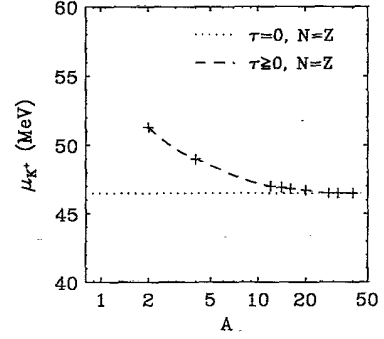


FIG. 1. Chemical potential for K^+ in MeV for central A on A collisions at 14.6A GeV/c. The crosses represent the values calculated using the NFS model. The dotted line is the value obtained by the program when complete stopping [$\tau=0$, see Eq. (7)] is assumed.

tively, where in larger systems $\pi^+/\pi^- \approx 1$. The Δ resonances in the reactions listed above subsequently decay into pions and nucleons. Their contribution is also listed in Table I. There are heavier mesons which can also be produced in similar reactions. Many of these mesons also decay into pions. We should stress at this point that the $p+p$ and $n+n$ reactions in Table I do not deliver results for the K/π ratios which could be compared to experimental data. This is because these very small systems with baryon number of 2 are very far from chemical equilibrium as assumed in a fireball model. We have only included them here to illustrate the isospin effect.

When transparency is taken into consideration, the temperature and chemical potential are no longer independent of A . For light nuclei, like helium, the nucleons retain 20% of their center-of-mass momentum. While the transparency has little effect on the pion chemical potential, it does affect the temperature and kaon chemical potential. While the temperature increases by 0.9% for d on d reactions to Si on Si, the kaon chemical potential decreases by 9.4%, as can be seen in Fig. 1.

IV. COMPARISON WITH EXPERIMENT

Data from experiments at AGS are available for Si projectiles on Al and Au targets at beam energies of 14.6A GeV. The detectors were triggered on central collisions. In our calculations, we considered collisions with impact parameters less than 2 fm as central [28]. The data are presented in two forms, the invariant cross section in the laboratory frame as a function of transverse mass and the rapidity distribution.

In Figs. 2 and 3, the invariant cross sections of p , π , and K at midrapidity calculated by the firestreak model are compared to those measured by the E802 Collaboration [29,30]. A nucleon-nucleon cross section of 40 mb was used for the transparency calculation. In the Si-Au system, this resulted in complete stopping of the projectile. In the lighter Si-Al system, the projectile was completely stopped for exactly central collisions, and only partially stopped for $b \neq 0$.

The pion spectra agree reasonably well with the data.

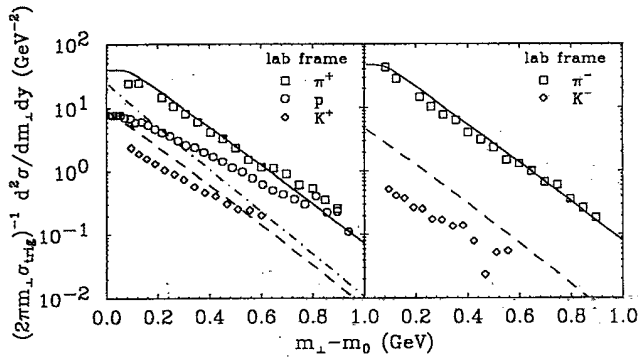


FIG. 2. Invariant cross sections of p , π^\pm , and K^\pm from 14.6A GeV Si+Au collisions for $1.2 \leq y \leq 1.4$. The data are taken from Ref. [29]. The lines represent the results [28] of the calculations with the modified firestreak model for p (dashed), π (solid), and K (dot-dashed).

A slight overprediction is observed in our model. The same effect is also observed in other model calculations [31]. A freeze-out density equal to that of normal nuclear matter has been used in our calculation. Decreasing the density below this value has the effect of increasing the slope of the spectra slightly. The model predicts the transverse mass distributions of the kaons and pions to have almost the same slope. Our model cannot reproduce the slope of the proton spectra. While increasing the freeze-out density would decrease the slope of the various spectra, the pion spectrum's slope never exceeds that of the proton as it does experimentally. We attribute this disagreement to the possible occurrence of collective baryon flow, which of course is not an ingredient of our model.

We can also observe that we consistently overpredict the kaon yield as compared to the data. This overprediction is due to the fact that our assumption of chemical equilibrium is only partially fulfilled. The amount by which we overpredict the data is a measure of how much the physical heavy ion collisions are off chemical equilibrium. One can of course obtain much better agreement with the data by introducing a kaon freeze-out density

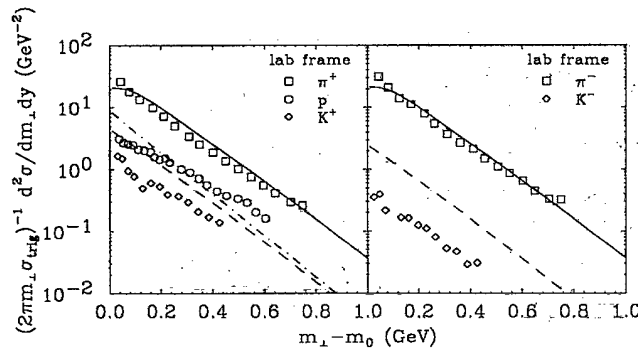


FIG. 3. Invariant cross section of p , π^\pm , and K^\pm from 14.6A GeV Si+Al collisions for $y = 1.5$. The data are taken from Ref. [30]. The lines represent the results [28] of the calculations with the modified firestreak model for p (dashed), π (solid), and K (dot-dashed).

TABLE II. K/π ratios for central A on B collisions at 14.6A GeV/c.

		$p + \text{Be}$	$p + \text{Au}$	Central Si + Au
K^+/π^+	NFS	14.7	12.5	26.3
	Expt	7.8	12.5	18.2
K^-/π^-	NFS	6.7	3.9	12.5
	Expt	2.0	2.8	3.2

which is independent of the pion freeze-out density. In this way the relative normalization of kaon and pion spectra can be adjusted. We opted not to use this additional fit parameter, because it is not the main purpose of this paper to fit data, but to work out systematic size effect in the K/π ratios.

By integrating the invariant cross sections over transverse mass, the rapidity distributions

$$\frac{dN}{dy} = \frac{1}{\sigma_0} \frac{d\sigma}{dy} \quad (36)$$

are found. In Fig. 4, these are compared to rapidity distributions extracted from experimental data where an exponential fit to the transverse mass spectra is assumed and then integrated [8]. For the model curves,

$$\sigma_0 = A_p \sigma_{\text{trig}} = 28(\pi b_{\text{max}}^2). \quad (37)$$

The K/π ratios at central rapidity are summarized in Table II for $p + A$ and Si+Au collisions. Both the experimental and model calculations produce K^+/π^+ ratios which exceed the K^-/π^- ratios. However, the model predictions exceed the experimental values by as much as a factor of 3.9 at this rapidity. The predictions for K^+/π^+ agree better with experiment. This is because of the larger production cross sections for K^+ than for K^- due to the associated production with hyperons, which brings K^+ closer to the chemical equilibrium assumed in our model.

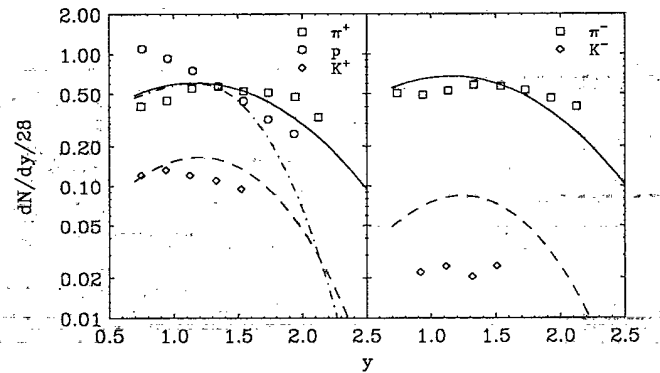


FIG. 4. Rapidity distributions for p , π^\pm , and K^\pm from central 14.6A GeV Si+Au collisions. The data are taken from Ref. [7]. The lines represent the results [28] of the calculations with the modified firestreak model for p (dashed), π (solid), and K (dot-dashed).

V. CONCLUSIONS

We have introduced a modified firestreak model for the calculation of production cross sections of strange mesons and baryons. This is done by inclusion of all strange and nonstrange mesons and baryons with masses of up to 1.3 GeV in the formalism. We have also provided a way to calculate geometric transparency and partial stopping in our framework.

We find that our model is successful in predicting available pion spectra at AGS energies ($E/A \approx 15$ GeV). Our model predicts complete stopping for Si projectiles and heavy targets such as Au, but for light targets such as Al, complete stopping occurs only for very central collisions.

Since our model is of purely thermal origin, it predicts the same temperature for all emitted particles, and is of course not able to reproduce the experimental fact that the apparent temperatures of emitted pions, kaons, and protons are different.

In our model, more than half (60–80 %) of the produced pions and kaons are of thermal origin, and only a small contribution is due to resonance decays.

We find that we systematically overpredict the kaon yields for all reactions considered. This is a good indication that kaons are not in chemical equilibrium in the experiments performed at AGS [32]. We attribute this to

the relatively small production cross sections of strange mesons at this beam energy, which make approaches based on chemical equilibrium somewhat questionable.

We do, however, find that we are able to reproduce the experimental findings that the K/π ratio is systematically higher (up to a factor of 5 in experiments) for the positively charged mesons than for the negatively charged ones. We are also able to reproduce the systematic increase of the K/π ratios from $p+A$ to $A+A$ systems, which is found in experiment. In our model, however, this dependence of the K/π ratio on the mass (baryon number) of the system is basically due to the fact that more energy per nucleon is available in the fireball generated in the collision of a symmetric (or almost symmetric) heavy ion system than in a proton-induced reaction at the same beam energy per nucleon. In addition, we find a small isospin effect: $n+n$ collisions have a higher K^+/π^+ ratio than $p+p$ collisions, and in heavier systems $n+n$ collisions become increasingly more probable.

It is therefore our conclusion that an increase in the K^+/π^+ ratio with the total mass of the heavy ion system can be caused by purely hadronic effects. An interpretation of the high K^+/π^+ ratio as a possible signal for the creation of a quark-gluon plasma then appears to be questionable.

- [1] J. Rafelski and B. Müller, *Phys. Rev. Lett.* **48**, 1066 (1982).
 [2] H. C. Eggers and J. Rafelski, *Int. J. Mod. Phys. A* **6**, 1067 (1991).
 [3] O. Hansen, *Comments Nucl. Part. Phys.* **20**, 1 (1991).
 [4] P. Koch, B. Müller, and J. Rafelski, *Phys. Rep.* **142**, 169 (1986).
 [5] T. Matsui *et al.*, *Phys. Rev. D* **34**, 783 (1986); **34**, 2047 (1986).
 [6] H. W. Barz, B. L. Friman, J. Knoll, and H. Schulz, *Nucl. Phys. A* **484**, 661 (1988).
 [7] Y. Miake *et al.*, E802 Collaboration, in *Proceedings of the Workshop on Heavy Ion Physics at the AGS*, edited by O. Hanson (Brookhaven National Laboratory, Upton, New York, 1990), p. 240.
 [8] T. Abbott *et al.*, E802 Collaboration, *Phys. Rev. Lett.* **66**, 1567 (1991).
 [9] K. S. Lee, M. J. Rhoades-Brown, and U. Heinz, *Phys. Rev. C* **37**, 1452 (1988).
 [10] J. Cleymans, H. Satz, E. Suhonen, and D. W. von Oertzen, *Phys. Lett. B* **242**, 111 (1990).
 [11] G. E. Brown, C. M. Ko, Z. G. Wu, and L. H. Xia, *Phys. Rev. C* **43**, 1881 (1991); C. M. Ko, Z. G. Wu, L. H. Xia, and G. E. Brown, in *Proceedings of the Workshop on Heavy Ion Physics at the AGS* [7], p. 361; *Phys. Rev. Lett.* **66**, 2577 (1991).
 [12] L. H. Xia, and C. M. Ko, *Phys. Lett. B* **222**, 343 (1989); *Nucl. Phys. A* **498**, 561c (1989); *Phys. Rev. C* **38**, 179 (1988).
 [13] B. L. Friman, *Nucl. Phys. A* **498**, 161c (1989).
 [14] S. Chapman and M. Gyulassy, *Phys. Rev. C* (to be published).
 [15] J. Stachel, in *Proceedings of the Workshop on Heavy Ion Physics at the AGS* [7], p. 144.
 [16] J. Stachel and P. Braun-Munzinger, *Nucl. Phys. A* **495**, 393c (1989).
 [17] R. Mathiello, H. Sorge, H. Stöcker, and W. Greiner, *Phys. Rev. Lett.* **63**, 1459 (1989).
 [18] W. Q. Chao, C. S. Gao, and Y. L. Zhu, *Nucl. Phys. A* **514**, 734 (1990).
 [19] M. Gyulassy, in *Proceedings of the Workshop on Heavy Ion Physics at the AGS* [7], p. 503.
 [20] N. S. Amelin *et al.*, *Phys. Rev. C* **44**, 1541 (1991).
 [21] K. Werner, *Phys. Lett. B* **219**, 111 (1989); *Z. Phys. C* **42**, 567c (1989).
 [22] H. Sorge, H. Stöcker, and W. Greiner, *Nucl. Phys. A* **498**, 567c (1989).
 [23] J. Gosset, J. I. Kapusta, and G. D. Westfall, *Phys. Rev. C* **18**, 844 (1978); W. D. Myers, *Nucl. Phys. A* **296**, 177 (1978).
 [24] T. Abbott *et al.*, *Phys. Lett. B* **197**, 285 (1987); P. Braun-Munzinger *et al.*, *Z. Phys. C* **38**, 45 (1988); M. S. Tannenbaum *et al.*, *Nucl. Phys. A* **488**, 555c (1988).
 [25] P. Danielewicz and J. M. Namyslowski, *Acta. Phys. Polon. B* **12**, 695 (1981).
 [26] K. K. Gudima and V. D. Toneev, *Yad. Fiz.* **42**, 645 (1985) [*Sov. J. Nucl. Phys.* **42**, 409 (1985)].
 [27] W. Bauer, *Phys. Rev. Lett.* **61**, 2543 (1988).
 [28] To match our results to the centrality trigger used in experiment we had to uniformly scale down all of our cross sections by a factor of 2. Any ratios of particle production cross sections were, of course, invariant under this rescaling.
 [29] B. Moskowicz *et al.*, E802 Collaboration, in *Advances in Nuclear Dynamics*, edited by W. Bauer and J. Kapusta (World Scientific, Singapore, 1991).
 [30] J. B. Costales *et al.*, E802 Collaboration, in *Proceedings of the Workshop on Heavy Ion Physics at the AGS* [7], p. 249.
 [31] C. M. Ko (private communication).
 [32] G. F. Bertsch, *Comments Nucl. Part. Phys.* **19**, 91 (1991).